



Original Articles

TCR-induced FOXP3 expression by CD8⁺ T cells impairs their anti-tumor activity

Teresa Lozano ^{a, **, 1}, Enrique Conde ^{a, 1}, Celia Martín-Otal ^a, Flor Navarro ^a, Aritz Lasarte-Cia ^a, Rabab Nasrallah ^c, Diego Alignani ^b, Marta Gorraiz ^a, Pablo Sarobe ^a, Juan P. Romero ^d, Amaia Vilas ^d, Rahul Roychoudhuri ^{c,e}, Sandra Hervás-Stubbs ^a, Noelia Casares ^a, Juan José Lasarte ^{a,*}

^a Immunology and Immunotherapy, Center for Applied Medical Research (CIMA), University of Navarra, 31008, IdISNA, Pamplona, Spain

^b Flow Cytometry Core, Center for Applied Medical Research (CIMA), University of Navarra, 31008, IdISNA, Pamplona, Spain

^c Laboratory of Lymphocyte Signalling and Development, Babraham Institute, Cambridge, UK

^d Oncohematology Programs, Center for Applied Medical Research (CIMA), University of Navarra, 31008, IdISNA, Pamplona, Spain

^e Division of Immunology, Department of Pathology, University of Cambridge, Cambridge, UK

ARTICLE INFO

Keywords:

FOXP3
NFAT
CD8⁺ T cells
Adoptive cell therapy

ABSTRACT

Adoptive cell transfer therapy using CD8⁺ T lymphocytes showed promising results eradicating metastatic malignancies. However, several regulatory mechanisms limit its efficacy. We studied the role of the expression of the transcription factor FOXP3 on CD8⁺ T cell function and anti-tumor immunity. Here we show that suboptimal T cell receptor stimulation of CD8⁺ T cells upregulates FOXP3 *in vitro*. Similarly, CD8 T cells transferred into tumor-bearing mice upregulate FOXP3 *in vivo*. Cell-intrinsic loss of FOXP3 by CD8⁺ T cells resulted in improved functionality after TCR stimulation and better antitumor responses *in vivo*. Inhibition of the FOXP3/NFAT interaction likewise improved CD8⁺ T cell functionality. Transcriptomic analysis of cells after TCR stimulation revealed an enrichment of genes implicated in the response to IFN-γ, IFN-α, inflammatory response, IL-6/JAK/STAT, G2M checkpoint and IL-2/STAT signaling in FOXP3-deficient CD8⁺ T cells with respect to FOXP3-wt CD8⁺ T cells. Our results suggest that transient expression of FOXP3 by CD8⁺ T cells in the tumor microenvironment restrains their anti-tumor activity, with clear implications for improving T cell responses during immunotherapy.

1. Introduction

Adoptive T cell transfer immunotherapy with *ex vivo*-expanded tumor-infiltrating lymphocytes (TILs) has achieved objective clinical responses in a significant proportion of cancer patients (reviewed in Ref. [1]). Failure to reach long-term tumor control in many patients is partially due to tolerization of transferred T cells in the tumor microenvironment [2] that may be governed by specific transcriptional regulatory networks [3].

FOXP3 is one of the transcription factors that influences overall T cell activation. FOXP3 controls the differentiation and function of regulatory T cells (Treg) generated in the thymus when self-antigens are presented by thymic stromal cells [4,5]. In addition to naturally occurring Tregs

(nTreg) generated in the thymus, FOXP3 expression can be induced in peripheral CD4⁺CD25[−] T cells through TCR crosslinking, leading to attenuation of their effector functions [6–10]. However, FOXP3 is not only expressed in CD4⁺ cells. CD8⁺ T cells can transiently express FOXP3 after TCR stimulation although there is some controversy surrounding its effect on T cell effector functions [11–14]. This could be particularly relevant in therapeutic strategies based on the adoptive cell transfer of antigen-specific CD8⁺ T cells. The conversion of CD8⁺ effector T cells into stable or transient FOXP3-expressing T cells may be one mechanism by which tumors prevent the anti-tumor immune response from effectively controlling tumor growth [15]. However, this process and the potential role of FOXP3 expression on CD8⁺ T cells remains poorly understood.

* Corresponding author. Immunology and Immunotherapy Program, Center for Applied Medical Research (CIMA), Avenida Pío XII, 55, 31008, Pamplona, Spain.

** Corresponding author. Immunology and Immunotherapy Program, Center for Applied Medical Research (CIMA), Avenida Pío XII, 55, 31008, Pamplona, Spain.

E-mail addresses: tmoreda@unav.es (T. Lozano), jjlasarte@unav.es (J.J. Lasarte).

¹ TL and EC contributed equally to this work.

Engagement of the TCR by its cognate antigen leads to the nuclear translocation of NFAT1, which forms a cooperative complex with AP-1 [16] and mediates the transcriptional regulation of several genes such as IL-2 [17]. However, NFAT1 can also promote CD8⁺ T cell exhaustion by binding sites that do not require cooperation with AP-1 [18,19]. In CD4⁺ T cells, FOXP3 orchestrates its functions through interaction with key transcription factors for T cell activity, including NFAT [20,21], NF-κB [22] and AML1 [23], together with an increasing number of protein partners in the so-called FOXP3 interactome [24]. Given that FOXP3 is readily detectable in human CD8⁺ T cells upon activation, it is important to establish its function in these cells. TCR-induced FOXP3 could bind to NFAT and elicit a suppressor/anergic program in CD8⁺ T cells. Our results on the effect of cell-intrinsic loss of FOXP3 by CD8⁺ T cells points to this transcription factor as a potential intracellular checkpoint inhibitor of CD8⁺ T cell activation and thus, a direct target for the improvement of anti-tumor CD8⁺ T cell immunity.

2. Materials and methods

2.1. Mice

C57BL/6J mice were obtained from Harlan (Barcelona, Spain). For adoptive T cell transfer studies, OT-1 TCR transgenic mice (C57BL/6-Tg (TcraTcrb)1100Mjb/J) (The Jackson Laboratory, ME, USA), whose T cell receptor is specific for the peptide OVA_{257–264} in the context of H2K^b, were used to obtain donor CD8⁺ T cells. Female Scurfy mice (B6. Cg-FOXP3sf^{+/+}/J, Scurfy), and CD45.1 transgenic BL/6 mice (B6.SJL-PtprcaPep3b/BoyJ mice) were purchased from the Jackson Laboratory and bred in our animal facilities under specific pathogen-free conditions. Female Scurfy mice were bred with male C57BL/6 mice to produce SF mice (FOXP3sf/Y). OT-1/CD45.1 mice were generated by breeding OT-1 mice with CD45.1 mice. OT-1 Scurfy mice were generated by breeding OT-1/CD45.1 males with B6.Cg-FOXP3sf^{+/+}/J female mice. B6-FOXP3^{EGFP}/B6.Cg-FOXP3^{tm2(EGFP)Tch}/J (FOXP3^{GFP} for short) reporter mice were purchased from the Jackson Laboratory. FOXP3^{GFP}OT-1/CD45.1 mice were generated by cross-breeding FOXP3^{GFP} mice with OT-1/CD45.1 mice.

The presence of the FOXP3sf mutation was confirmed by PCR as described on the Jackson Laboratory's web site by using FOXP3 sequencing and flow cytometry to measure the lack of expression of FOXP3 (Mouse regulatory T cell staining kit, eBiosciences). The presence of the OT-1 TCR transgene was confirmed by staining with Class I iTAG MHC Tetramers (Beckman Coulter) specific for the SIINFEKL peptide bound to MHC. Mice were examined twice weekly for clinical signs of immune dysfunction, including skin inflammation, weight loss, wasting, among other features. All animal handling and tumor experiments were conducted under the institutional guidelines of our institutional ethics committee (protocols R-131.16, R-018-19) and 2019.162).

2.2. Cell lines

The murine melanoma B16F10 expressing the OVA (B16-OVA) cell line (obtained from Dr. G. Kroemer; Paris, France) was cultured in mouse medium (RPMI 1640, 10% Fetal Calf Serum (Sigma), 100 U/ml penicillin and 100 µg/ml streptomycin (Invitrogen), 10 mg/ml Gentamicin (Gibco)). The retroviral packaging cell line Platinium-E (Invitrogen) was cultured in DMEM containing 10% FBS, antibiotics, 2 mM glutamine and 50 µM beta-mercaptoethanol, and supplemented with 10 µg/ml blasticidin and 1 µg/ml puromycin (Gibco). All cell lines were cultured at 37 °C in a humidified atmosphere with 6.5% CO₂.

2.3. Blood samples

Peripheral blood mononuclear cells (PBMC) were obtained from fresh heparinized blood samples from human healthy donors by Ficoll-Paque centrifugation. CD8⁺ T cells were purified by negative selection

using the CD8⁺ T cell isolation kit (Miltenyi) according to the manufacturer's instructions. Cells were cultured in 96-well round-bottomed plates (10⁵ cells/well) in the presence or absence of anti-CD3/CD28 beads (Gibco) at the indicated cell:beads ratios with IL-2 (100 IU/ml). The IFN-γ released to the culture supernatant was measured by ELISA (R&D System). FOXP3 expression was measured by flow cytometry using anti human FOXP3 antibody (eBiosciences). In some experiments, TGF-β (5 ng/ml, Peprotech) was added and cultured for 5 days to measure FOXP3 expression. The study was conducted according to the guidelines of the Declaration of Helsinki, and approved by the Institutional Ethics Committee of the Universidad de Navarra (protocols R-131.16 (Ref 2019.162).

2.4. Plasmids and retroviral transduction

The retroviral expression plasmids KMV IRES-GFP and MSCV IRES-GFP encoding myc tagged FOXP3 were kindly provided by Dra A. Rao (La Jolla, USA). The plasmid encoding FOXP3 peptide 393-403 (MKCFVREVESEKGA) was generated by cloning the sequence ggccgcacatggAAARGTTTGTAAGAGTAGAAAGTAAAAAGGAGCAtaa into the NotI and SalI restriction sites within MSCV-IRES-GFP.

Retroviral CRISPR-Cas9 expressing sgRNAs to target Foxp3 were generated by using pRubiG-T2A-Cas9 plasmid where the ubiquitin promoter expresses GFP and humanized spCas9 (PX330) linked via a T2A motif (Addgene Plasmid #75348, deposited by Bryan Luikart). We inserted the U6 promoter and two different sgRNAs for Foxp3 into the Pac1 and BstB1 sites. Thus, the retrovirus RVRubi-E6Foxp3 encoding chimeric single guide RNA (sgRNA) containing short sequences homologous to Foxp3 exon 5 (sg1: GGACCTAGTCGGGCCAGA) or exon 6 (sg2:GGTTGTCCAGTGGACCGACT) and the sequences necessary for Cas9 interaction were generated. sgRNA were selected from the Mouse GeCKO v2 library designed by Feng Zang's laboratory (<https://www.addgene.org/pooled-library/zhang-mouse-gecko-v2/>). Gene editing efficiency was evaluated analyzing indel percentage using TIDE (Tracking of Indels by DEcomposition) webtool [25]. The retrovirus RVRubi expressing only Cas9 was used as control.

Platinum-E ecotropic packaging cells (Cell Biolabs) were plated 1 day before transfection in 6-well plates (Becton Dickinson) at 10⁶ cells/well. They were transfected with 5 µg of retroviral plasmid DNA along with 2.5 µg of pCL-Eco plasmid DNA using lipofectamine 2000 (Invitrogen) for 8 h in antibiotic-free medium. Retroviral supernatants were collected at 48 and 72 h and spun at 2,000 × g for 90 min at 32 °C into 12-well plates containing mouse CD8⁺ T cells pre-activated for 24 h with αCD3/CD28-coated beads (BD). Lymphocytes were cultured with 100 IU/ml recombinant human IL-2.

2.5. Antibodies and flow cytometry

The following fluorochrome-conjugated antibodies recognizing surface antigens were used at 0.25–1 × 10⁻³ mg/ml: CD8a (53–6.7), CD4, (RM4-5) CD45.1 (A20), CD45.2 (104), CD25 (PC61), CD44 (IM7), CD62L (MEL-14), CD137 (17B5), PD-1 (29F.1A12), KLRG1 (2F1), CD69 (H1.2F9), LAG3 (C9B7W), and tetramer for SIINFEKL-H2Kb. For staining, cells were incubated with the Zombie NIR™ Fixable Viability kit (Biolegend) for 15 min at room temperature and then washed once with washing buffer (PBS without Ca/Mg, 0.5 M EDTA, 10% of Fetal Bovine serum and 1% Penicillin/streptomycin). Subsequently, cells were incubated with specific antibodies for 30 min on ice in the presence of 2.4G2 monoclonal antibody (mAb) to block FcγR binding. Cells were fixed and permeabilized with the FOXP3/Transcription Factor Staining kit buffers (eBiosciences) and then stained intracellularly (15 min, RT) with fluorochrome-conjugated mAbs against mouse Ki67 (16A8), TNF-α (MP6-XT22), IFN-γ (XMG1.2) and FOXP3 (FJK-16s). Data acquisition was performed with a FACS Canto II flow cytometer (Becton Dickinson) and analyzed by FlowJo software (TreeStar). Perfect-Count beads (Cytognos) were added for the flow cytometric quantification of

absolute cell numbers. All analyses were performed after gating on live single cells.

2.6. Quantitative reverse-transcription polymerase chain reaction (*qRT-PCR*)

Cells were isolated by flow cytometric sorting (BD FACSAria™ IIu sorter) or by magnetic separation, harvested and transferred to Lysis/binding solution (Ambion) for storage at -80°C . Total RNA from pelleted cells was isolated using the MagMax 96 total kit (Ambion). One microgram of RNA was treated with DNase I and retrotranscribed to cDNA with M-MLV RT in the presence of RNase OUT (Invitrogen, Carlsbad, CA). For real-time PCR reactions, 1 μl of cDNA was incubated with specific primers using iQ SYBR Green Supermix (Bio-Rad, Hercules, CA). β -Actin was used to normalize gene expression. mRNA values were represented by the formula: $2^{\Delta C_t}$, where ΔC_t indicates the difference in the threshold cycle between β -Actin and the target genes.

2.7. Protein-protein interaction assays

The MicroScale Thermophoresis (MST) assay was carried out to study FOXP3/NFAT interaction. NFAT protein (80 μM) labelled with a RED dye (RED-NHS-2nd generation labelling kit, NanoTemper) was incubated for 2 h with different concentrations of the forkhead domain of FOXP3 (FKH-FOXP3) or an irrelevant control protein (from 30 μM to 1 nM) and analyzed by microscale thermophoresis (Monolith Nano-Themper). Protein-protein interaction kD was quantified by using the Monolith software.

The proximity ligation assay was performed to visualize the *in situ* endogenous FOXP3/NFAT interaction and its localization in the cell. 293 cells were transfected with FLAG-FOXP3 or HA-NAFT expressing plasmids alone (as negative controls) or in combination (0.2 μg each). Forty-eight hours later, cells were fixed with 4% paraformaldehyde and permeabilized with 0.25% Triton in PBS. After blockade of non-specific binding, mouse-anti HA (Sigma, H3663) and rabbit -antiFLAG (Sigma, F7425) antibodies (1/300 dilution) in antibody buffer. After washing, labelled secondary antibodies were added to perform the amplification process according to the manufacturer's instructions (Duolink PLA, Sigma). After the addition of fluorescent probes, cells were visualized by fluorescent microscopy. The DAPI staining solution was used for nuclear staining.

2.8. Real-time cytotoxicity assay

A Real-time cytotoxicity assay (xCELLigence) was carried out to analyze the cytotoxicity of CD8 $^{+}$ cells modified with retrovirus RV-ppt393 (expressing the peptide F393-403 inhibitor of FOXP3/NFAT interaction [10]). Background impedance signal was measured with 50 μL cell culture medium per well on E-Plates 96 (Roche, Grenzach-Wyhlen, Germany). Subsequently, target cells were seeded in an additional 100 μl of medium at a density of 20,000 cells per well. Cell attachment was monitored using the RTCA SP (Roche) instrument and the RTCA software Version 1.1 (Roche) until the plateau phase was reached, which was usually after approximately 18 h. CD8 $^{+}$ T cells were added at different Effector:Tumor ratios ranging from 0.1:1 to 0.2:1. Upon addition of effector cells, impedance measurements were monitored in real-time every 10–30 min during the 48 h the culture lasted. Changes in electrical impedance were expressed as a dimensionless cell index (CI) value, which derives from relative impedance changes corresponding to cellular coverage of the electrode sensors, normalized to baseline impedance values with culture medium only.

2.9. Mixed bone marrow chimeras

For bone marrow (BM) reconstitution experiments, CD45.1 C57BL/6 J mice received 10 Gy total-body γ -radiation (TBI) from a ^{137}Cs source

before being intravenously injected with mixed BM cells from: (i) Scurfy CD45.2 $^{+}$ and from CD45.1 $^{+}$ donor mice at a 1:1 ratio (to generate the Foxp3 $^{\text{Scurfy}}$ chimera mice); (ii) CD45.2 $^{+}$ C57BL/6 J and from CD45.1 $^{+}$ donor mice (to generate the control Foxp3 $^{\text{wt}}$ chimeras). To generate OT-1 TCR transgenic bone marrow chimeras, CD45.2 $^{+}$ C57BL/6 J mice were irradiated (10 Gy TBI) before being intravenously injected with a mixed BM cells from (iii) OT-1 Foxp3 $^{\text{Scurfy}}$ CD45.1 $^{+}/2^{+}$ and from CD45.2 $^{+}$ donor mice at a 1:1 ratio (to generate the OT-1 Foxp3 $^{\text{Scurfy}}$ chimeras), and (iv) from OT-1 Foxp3 $^{\text{wt}}$ CD45.1 $^{+}/2^{+}$ and from CD45.2 $^{+}$ donor mice (to generate the corresponding control OT-1 Foxp3 $^{\text{wt}}$ chimeras). The bone marrow from 6 to 10-week-old donor mice was used except with Scurfy or OT-1 Scurfy mice where 18 days old pups were used as donors.

2.10. Adoptive cell transfer experiments in tumor-bearing mice

Eight-week-old C57BL/6 J mice ($n = 5$ –8 per group) were injected subcutaneously with 5×10^{5} B16-OVA melanoma cells on day 0. When the tumors had reached a diameter of 5×5 mm (day 5) the mice received a 300 rad total body irradiation (TBI) (Gammacell 3000 ELAN equipment, MDS Nordion) and were treated by adoptive transfer of the indicated CD8 $^{+}$ cells. Mice were treated with 4 intraperitoneal injections of recombinant human IL-2 (2×10^{5} IU) twice daily for 4 days after the T cell infusion. To characterize the transferred CD8 $^{+}$ cells, mice were sacrificed seven days after transfer and flow cytometry was used to evaluate the function, phenotype and number of tumor-infiltrating CD8 $^{+}$ T cells. ELISPOT assays were also performed to measure the number of tumor-specific IFN- γ producing cells in the spleen following the manufacturer's instructions (BD).

The therapeutic efficacy of adoptive cell therapies was measured by monitoring tumor size, by measuring the two perpendicular diameters with a caliper. The tumor area was calculated using the formula $A = (\text{length} \times \text{width})$. Mice were sacrificed when tumor covered an area greater than 2 cm^2 .

2.11. RNA-Seq analysis

Naïve CD8 T cells (CD62L $^{+}$ CD44 $^{-}$) from OT-1 Foxp3 $^{\text{Scurfy}}$ chimeras and from control OT1 Foxp3 $^{\text{wt}}$ chimeras were sorted by flow cytometry. Briefly, total CD8 $^{+}$ T cells were pre-enriched from single cell spleen suspensions using magnetic negative selection (Miltenyi) prior to FACS sorting using a MoFlo Astrios cell sorter (Beckman Coulter). Purified cells were then stimulated with 1 ng/ml of SIINFEKL peptide for 6 h before conducting the transcriptomic analysis. Briefly, 30000 cells were sorted into 100 μl of Lysis/Binding Buffer (Ambion), vortexed and stored at -80°C until further processing. Poly-A RNA was selected with Dynabeads Oligo (dT) (Ambion) and reverse-transcribed with Affinity-Script Multiple Temperature Reverse Transcriptase (Agilent) using poly-dT oligos carrying a 7 bp-index. Up to 8 samples with similar overall RNA content were pooled together and subjected to linear amplification by IVT using the HiScribe T7 High Yield RNA Synthesis Kit (New England Biolabs). Next, aRNA was fragmented into 250–350 bp fragments with RNA Fragmentation Reagents (Ambion) and dephosphorylated with FastAP (Thermo) following the manufacturer's instructions. Partial Illumina adaptor sequences (Jaitin, 2014) were ligated with T4 RNA Ligase 1 (New England Biolabs), followed by a second RT reaction. Full Illumina adaptor sequences were added during the final library amplification with KAPA HiFi DNA Polymerase (Kapa Biosystems). RNA-seq library quality controls consisted of quantification with a Qubit 3.0 Fluorometer (Life Technologies) and size profile examination with Agilent's 4200 TapeStation System. Libraries were sequenced in an Illumina NextSeq 500 system at a sequence depth of 10 million reads per sample.

RNA-seq reads were trimmed using Trim Galore v0.4.4 using the default parameters to remove the Nextera adapter sequence. Mapping was performed using STAR (2.6) against the mouse NCBI37 genome, guided by gene models from Ensembl annotation release 68.

Quantification and generation of gene expression matrices were performed with the function *featureCounts*, implemented in the R package Rsubread. Aligned fragments were imported into RStudio and prior to statistical analysis, the *filterByExpr* function, as implemented in the R package edgeR, was used to determine genes with sufficient counts to warrant further analyses. Differential gene expression analysis was performed using the DESeq2 algorithm within R and RStudio. Gene set enrichment analysis was carried out using GSEA software (<https://www.gsea-msigdb.org/>).

2.12. Statistical analysis

Statistical analyses were carried out using Graphpad Prism software, using either two-tailed Student *t* tests, one-way ANOVA or two-way ANOVA with the Bonferroni multiple comparison test (two tails), as indicated. Where necessary, the Shapiro–Wilk test was used to test for normality of the underlying sample distribution. Sample sizes were determined using power calculations based on the variability observed in previous experiments or based on previous experience of sample size requirements. Differences in survival were assessed using the Mantel–Cox log-rank test.

3. Results

3.1. CD8⁺ T cells express FOXP3 after suboptimal TCR stimulation

TCR stimulation of murine naïve CD44⁻CD62L⁺CD4⁺ T cells with αCD3 antibodies over four days induced the expression of FOXP3 in a large proportion of cells. This FOXP3 expression was significantly reduced when T cells were co-stimulated with αCD28 and, as has been found in previous reports, it was dramatically upregulated when TGF-β was added to the cultures ([6,26], Suppl Figure 1a). This induced FOXP3 expression was also observed in CD8⁺ T cells after TCR stimulation. A significant percentage of highly purified naïve CD8⁺ T cells from OT-1-FOXP3^{GFP} transgenic mice expressed FOXP3 when stimulated with suboptimal doses (0.001 ng/ml) of the cognate OVA257-264 (SIINFEKL) peptide (Fig. 1a). FOXP3 expression was gradually lost when the antigen concentration increased and this expression is transcriptionally regulated, as shown in the RT-PCR experiments (Fig. 1b). This down-regulation of FOXP3 expression correlated inversely with IFN-γ production in response to antigen stimulation (Fig. 1c). A kinetic analysis at 24, 48, 72 and 96 h confirmed this Foxp3 upregulation, particularly at antigen doses below 0.1 ng/ml (Suppl Fig 2A). The analysis of FOXP3 mRNA levels suggests a transient expression profile with a peak at 48 h (Suppl Fig 2B).

As described for CD4⁺ T cells, and in agreement with a previous work [14], TCR stimulation of CD8⁺ T cells in the presence of TGF-β enhanced FOXP3 expression. Using CD8⁺ T cells from OT-1 FOXP3^{GFP} mice, we observed that almost 50% of CD8⁺ T cells cultured in the presence of IL-2 and TGF-β became CD8⁺FOXP3⁺ cells after TCR stimulation with 0.1 ng/ml of the SIINFEKL peptide. This conversion was impaired when an ERK inhibitor was added to the culture, suggesting that FOXP3 expression is dependent on TCR stimulation (Fig. 1d–e). Importantly, those FOXP3⁺ CD8 T cells did not produce IFN-γ after brief stimulation with PMA/Ionomycin (Fig. 1f–g). Similar results were observed when CD8⁺ T cells were stimulated with αCD3 and TGF-β (Suppl Fig. 1b–c).

These results were reproduced using human CD8⁺ T cells from healthy donors. When purified CD8⁺ T cells from six healthy donors were stimulated with αCD3/CD28 beads, a significant percentage of CD8⁺ T cells (ranging from 4 to 15% depending on the donor) expressed FOXP3 (Fig. 1h). A titration assay with CD8⁺ T cells from three of these donors showed that FOXP3 expression peaked at an αCD3/CD28 beads to T cell ratio of 1:4 and gradually decreased as the beads:T cell ratio increased (Fig. 1i). FOXP3 downregulation at higher beads:T cell ratios inversely correlated with the production of IFN-γ suggesting that FOXP3 might impair the functionality of CD8⁺ T cells (Fig. 1j). As observed with

murine cells, FOXP3 upregulation was higher when human CD8⁺ T cells were stimulated with αCD3 in the presence of TGF-β, and inhibited when an ERK inhibitor was added to the culture (Fig. 1k). Taken together, these results suggest that suboptimal TCR stimulation acts in conjunction with TGF-β signaling to induce FOXP3 expression on human and murine CD8⁺ T cells.

3.2. Anti-tumor CD8⁺ T cells upregulate FOXP3 in vivo when recruited into the tumor

FOXP3^{GFP} mice were challenged with B16-OVA melanoma cells and 15 days later, when tumors reached 8–9 mm, they were sacrificed to analyze by flow cytometry the expression of FOXP3 in activated (CD137⁺) CD8⁺ T cells isolated from the spleen, lymph nodes, and tumors. Animals with no tumor were used as controls. We did not detect CD8⁺FOXP3⁺ T cells in the spleens or lymph nodes of control “tumor-free” mice, or in the spleens of tumor-bearing mice. However, a significant number of CD137⁺CD8⁺FOXP3⁺ T cells were found in the tumor and in the tumor-draining lymph nodes (Fig. 2a). The gating strategy on CD45live single CD8 cells and FOXP3^{GFP} intracellular expression and representative flow cytometry plots are shown in Suppl Fig. 3a and 3b respectively.

It has been reported that a proportion of CD8⁺ cells become FOXP3⁺ after their adoptive transfer into tumor bearing mice, probably due to exposure to signals such as TGF-β in the tumor microenvironment [15, 27]. We adoptively transferred CD8⁺ T cells from OT-1 CD45.1 mice (expressing the allelic marker CD45.1) into CD45.2 mice bearing OVA-expressing tumors. Five days after transfer, we found that CD45.1 T cells isolated from the tumor, but not from the spleen, upregulated FOXP3. Furthermore, CD8⁺ T cells isolated from tumors also upregulated IL-10 and LAG3 mRNA suggesting an impairment in their anti-tumor effector functions (Fig. 2b). These data suggest that the tumor microenvironment favors FOXP3 expression in anti-tumor CD8⁺ T cells.

3.3. Ectopic expression of FOXP3 on CD8⁺ T cells impairs their function in vitro

As reported for CD4⁺ T cells [28], FOXP3 expression in CD8⁺ T cells might repress effector cell functions. We found that ectopic over-expression of FOXP3 in OT-1 CD8⁺ T cells via retroviral infection reduced their functionality. Phenotypically, FOXP3 expression in CD8⁺ T cells (CD8⁺FOXP3⁺) upregulated CD25 and the immunosuppressor genes CTLA4 and IL-10, and reduced the expression of granzyme B compared to T cells transduced with control RV-GFP (CD8⁺GFP) (Fig. 2c and d). FOXP3 expression impaired CD8⁺ T cell proliferation and IFN-γ production in response to αCD3 or SIINFEKL peptide stimulation (Fig. 2e–f). This lower proliferative capacity was also observed when the expression of Ki67 was measured (Fig. 2g).

3.4. Inhibition of NFAT/FOXP3 interaction in activated CD8⁺ T cells improves T cell proliferation, cytokine production and lytic activity

The regulatory capacity of FOXP3 is to a large extent based on its ability to physically interact with NFAT and regulate its activity [21,22]. A biochemical assay of interaction based on microscale thermophoresis (MST) using recombinant NFAT protein labelled with a RED dye (Protein Labeling Kit RED-NHS, NanoTemper) and the FKH domain of Foxp3 demonstrated a specific NFAT:Foxp3 protein-protein interaction with a kD of around 1.68×10^{-7} M (Suppl Fig 4A). We also carried out a proximity ligation cell-based assay (PLA) in 293 cells transfected with plasmids expressing FLAG-Foxp3 and HA-NFAT plasmids. After 48 h of transfection, we visualized the subcellular location of NFAT:FOXP3 complexes using anti-FLAG and anti-HA antibodies. Using this assay, we observed NFAT-FOXP3 complexes both into the cytoplasm and in the nucleus of the cell (Suppl Fig 4B) suggesting that FOXP3 might facilitate the nuclear retention of NFAT [29] and influence NFAT DNA-binding

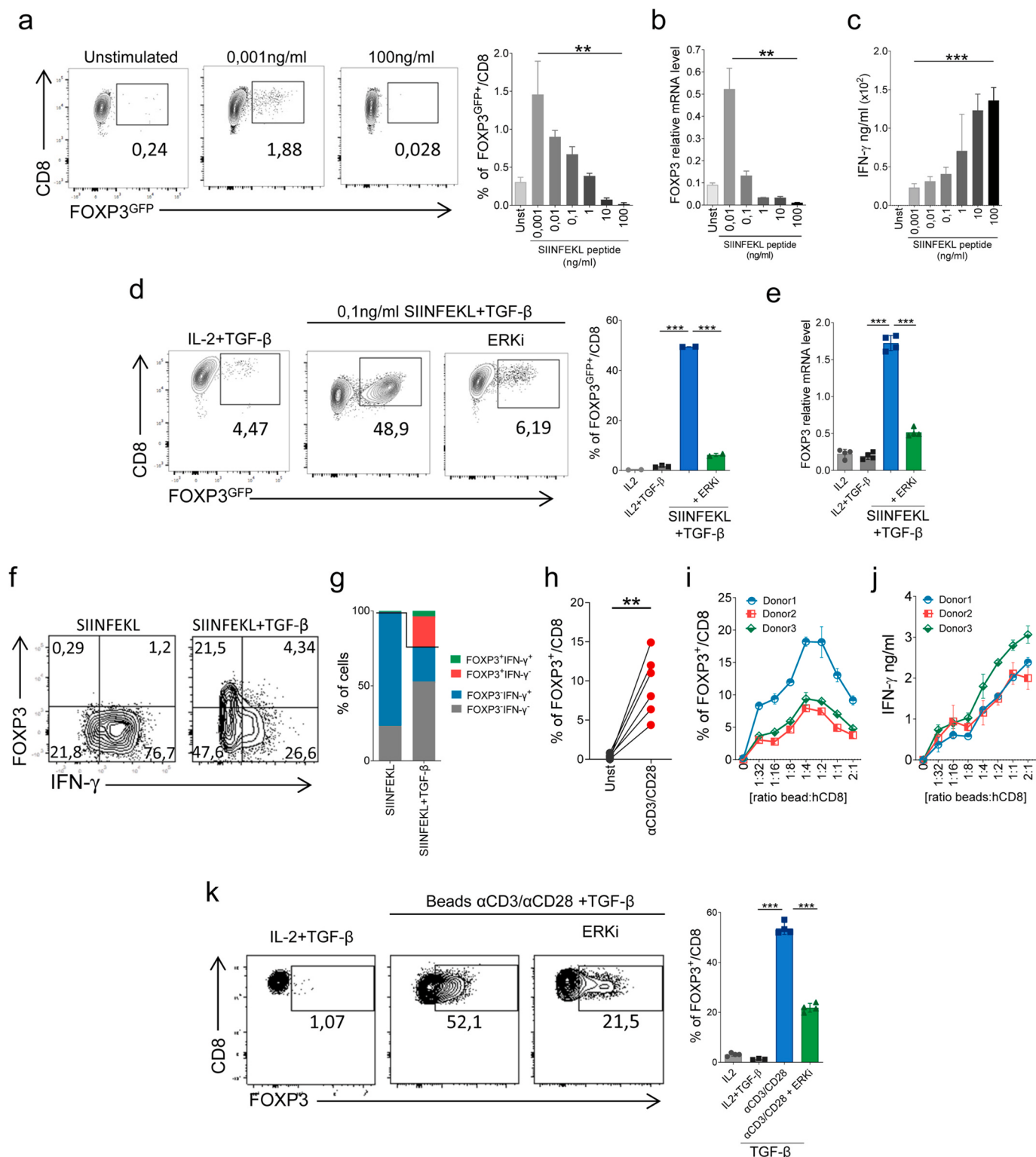


Fig. 1. CD8⁺ T cells express FOXP3 after suboptimal TCR stimulation or after stimulation in the presence of TGF-β. (a) Flow cytometry of CD8⁺ T cells isolated from OT-1xFOXP3^{GFP} mice and stimulated with SIINFEKL peptide at different concentrations (100–0,001 ng/ml) for 5 days. Percentage of FOXP3^{GFP} CD8⁺ T cells at day 5 (a-right) and FOXP3 expression after 12 h of stimulation as measured by qPCR (b). (c) IFN-γ production after 48 h of SIINFEKL stimulation. (d) Flow cytometry of naive CD8⁺ T cells isolated from OT-1xFOXP3^{GFP} mice and cultured in the presence of SIINFEKL (0.1 ng/ml) plus TGF-β (5 ng/ml) and ERK inhibitor (PD184352 at 3 μM) for 5 days. Percentage of GFP⁺ CD8⁺ T cells (d-right) and FOXP3 expression after 24h of culture as measured by qPCR (e). (f) Flow cytometry exemplifying the correlation between FOXP3 expression and IFN-γ production on CD8⁺ T cells. (g) Percentages after brief stimulation with PMA/Ionomycin at day 5 of culture. (h, i) Percentage of FOXP3⁺ cells in human CD8 T cells (n = 6 healthy donors) after 48 h of stimulation with αCD3/αCD38 beads at a 1:1 (h) or a different cell/bead ratio (n = 3 donors) (i) with simultaneous measurement of IFN-γ production by ELISA (j). (k) Flow cytometry of human CD8⁺ T cells cultured in the presence of αCD3/αCD28 beads (ratio 1:1) plus TGF-β (5 ng/ml) and ERK inhibitor (PD184352 at 3 μM) for 5 days. Data are representative of two independently repeated experiments (n = 3–6). Numbers in gates indicate percentages. **p < 0,01, ***p < 0,005. One-way ANOVA with Bonferroni multiple comparison test (b, c, e, k), paired Student ttest (h). Bars and error represent the mean and the SEM.

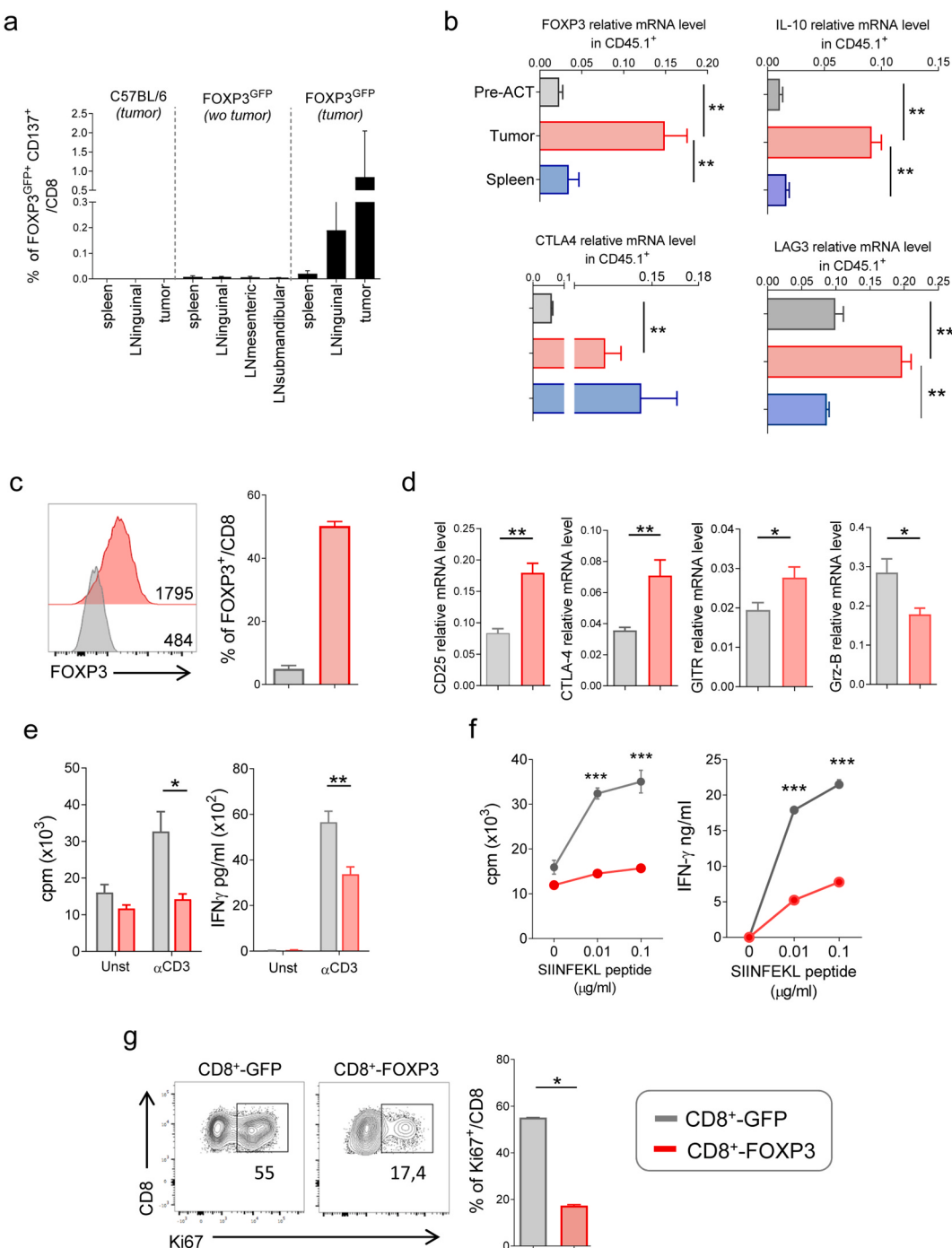


Fig. 2. CD8^+ T cells isolated from tumor and from tumor draining lymph nodes upregulate FOXP3. (a) C57BL/6 wild type and FOXP3^{gfp} mice ($n = 3$ mice per group) were challenged with B16-OVA tumor cells and 15 days later, CD8 T cell from the spleen, tumor draining lymph nodes and from tumors were analyzed by flow cytometry the percentage of $\text{FOXP3}^+ \text{CD137}^+$ cells. Mice without tumors were used as controls (wo tumor). (b) FOXP3, IL-10, CTLA4 and LAG3 expression on CD8 OT-1CD45.1 T cells five days after their injection into B16-OVA-bearing mice (qPCR on CD45.1^+ FACS-sorted cells) ($n = 3$ mice per group) (Pre-ACT: before adoptive cell transfer). (c–g) Ectopic expression of FOXP3 on CD8 T cells impairs their function *in vitro*: CD8⁺ T cells isolated from C57BL/6 mice were transduced with RV-FOXP3 or with RV-GFP retroviruses. (c) FOXP3 expression after retroviral infection expressed as geometric mean and percentage. (d) mRNA expression of Grz-B, CD25, CTLA-4 and GITR at day 6 after retroviral transduction. (e) Proliferation and IFN- γ analysis of transduced CD8 cells after two days of stimulation in coated plates with a low dose of αCD3 (50 ng/ml). (f) Proliferation and IFN- γ production of transduced CD8 OT-1 cells after 2 days of stimulation with the SIINFEKL peptide. (g) Frequency and percentage of Ki67⁺ T cells. Data are representative of two independently repeated experiments. Numbers in gates indicate percentages. * $p < 0.05$, ** $p < 0.01$, *** $p < 0.005$. Bars and error represent the mean and the SEM.

sites and target gene activation [17,21]. In a previous study, we identified a short synthetic peptide (FOXP3-393) able to inhibit FOXP3/NFAT interaction. This peptide impaired the suppressor activity of conventional Tregs and upregulated effector CD4⁺ T cell functions in response to TCR stimulation [10]. Consistent with this finding on CD4⁺

T cells, we found that FOXP3-393 improved proliferation and IL-2 production of naïve CD8⁺ T cells in response to suboptimal doses of αCD3 stimulation (Suppl Figure 5a).

In order to better inhibit FOXP3/NFAT interactions in CD8⁺ T cells, we produced a recombinant retrovirus (RV-ppt393) to intracellularly

express the FOXP3-393 peptide, by cloning a minigene coding for the peptide upstream of the IRES-GFP cassette. Purified CD8⁺ T cells were infected with RV-ppt393 or with a control retrovirus expressing GFP alone (RV-GFP) and seven days later, we studied the proliferative capacity and the production of IL-2 and IFN- γ in these cells in response to α CD3 antibody stimulation. RV-ppt393 transduced CD8⁺ T cells showed significantly improved cell proliferation, and IL-2 and IFN- γ production in response to α CD3 stimulation *in vitro* (Fig. 3a). Similar results were found when CD8⁺ T cells purified from OT-1 transgenic mice were transduced with RV-ppt393 (CD8⁺-ppt393) and stimulated with the SIINFEKL peptide (Fig. 3b) or when CD8⁺ T cells from Pmel transgenic mice were RV-ppt393 transduced and stimulated with a low dose (0.6 μ g/ml) of their cognate melanoma gp100 peptide (Suppl. Figure 5b). In agreement with these data, OT-1 CD8⁺-ppt393 T cells produced higher

IFN- γ levels when co-cultured with B16-OVA cells (Fig. 3c) and showed a greater capacity to kill B16-OVA cells *in vitro* (Fig. 3d). These results suggest that the FOXP3 inhibitory capacity on CD8⁺ T cells may be driven, at least in part, by its interaction with NFAT.

3.5. FOXP3-deficient CD8⁺ T cells exhibit enhanced *in vitro* functionality in response to TCR stimulation

We aimed to evaluate the impact of silencing FOXP3 on the functionality of naïve CD8⁺ T cells after antigen encounter. We first studied the effect of FOXP3 silencing on T cell function by using the CRISPR-Cas9 approach. We therefore engineered a retroviral CRISPR-Cas9 encoding chimeric single guide RNA (sgRNA) containing a short sequence homologous to the FOXP3 exon 6. The retrovirus RVRubi

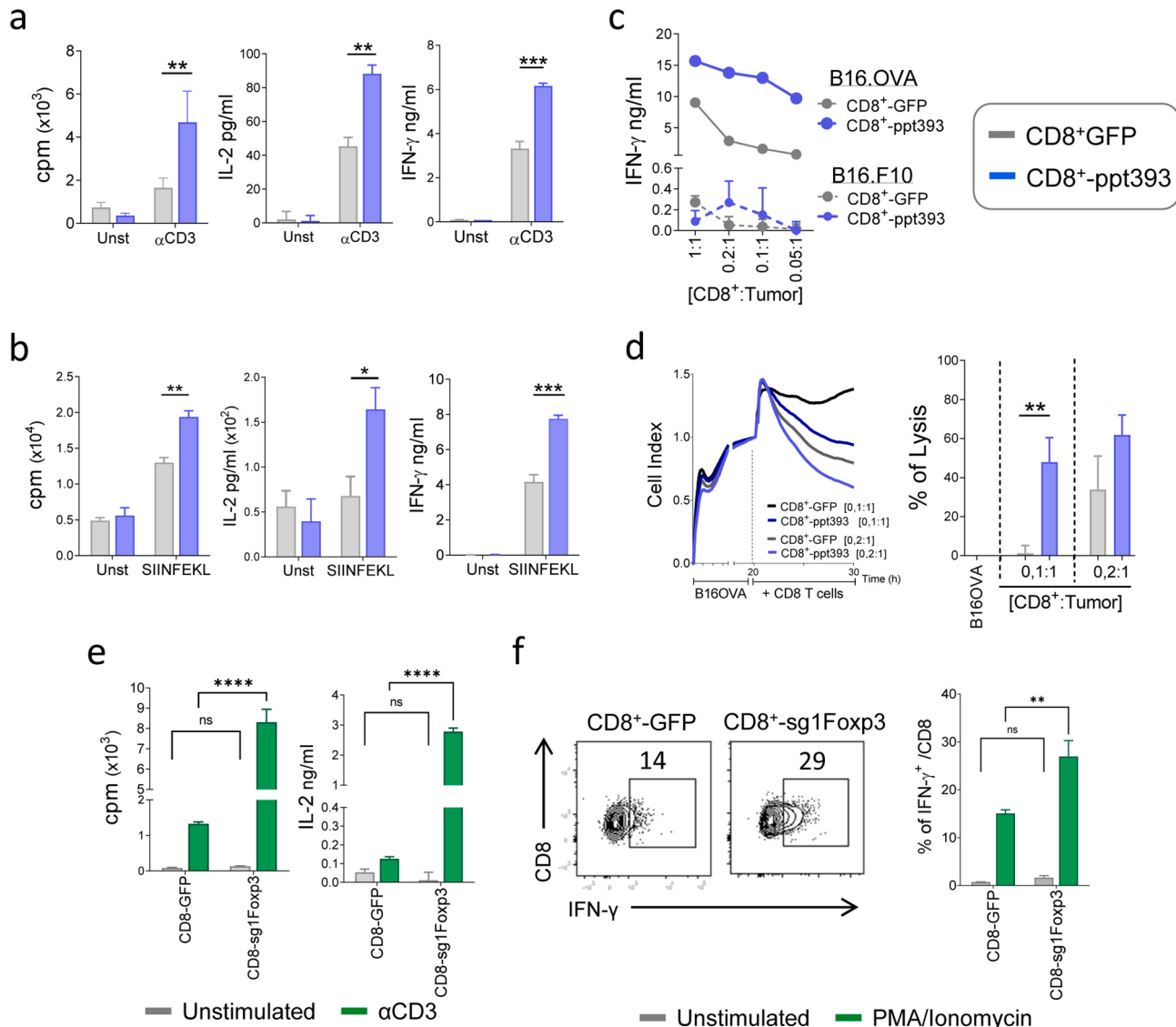


Fig. 3. Inhibition of NFAT/FOXP3 interaction or FOXP3 silencing in activated CD8⁺ T cells improves T cell proliferation, cytokine production and lytic activity. (a-b) CD8 T cell proliferation, IL-2 and IFN- γ production after 48h of stimulation. (a) CD8⁺ T cells from C57BL/6 J mice were transduced with RV-ppt393 or RV-GFP and activated using α CD3 coated plates (50 ng/ml). (b) CD8⁺ T cells from OT-1 mice were retrovirally transduced and stimulated with SIINFEKL peptide at (0.1 ng/ml). (c-d) Tumor reactivity of modified OT-1 CD8⁺ T-cells in co-culture with B16-OVA or with B16F10 tumor cells to measure IFN- γ production after 48h (e) Cytolytic activity of CD8⁺ T cells transduced with RV-ppt393 or RV-GFP measured by xCELLigence using B16-OVA as target cells at different CD8⁺: target cell ratios (d). (e, f) Retroviral transfection with CRISPR-Cas9 targeting FOXP3 enhances their function in response to TCR stimulation *in vitro*. (e) Murine CD8⁺ T cells were retrovirally transduced with RV-GFP or with RV-sg1FOXP3 and stimulated with α CD3 to measure T cell proliferation and IL-2 production. (f) Intracellular cytokine staining of IFN- γ after brief stimulation with PMA/Ionomycin. Numbers in gates indicate percentages. Data are representative of two independently repeated experiments ($n = 3-4$). * $p < 0.05$, ** $p < 0.01$, *** $p < 0.005$, ns = no statistically significant differences. Two-way ANOVA with the Bonferroni multiple comparisons test (a, b, d, e and f). Bars and error represent the mean and the SEM.

expressing only Cas9 was used as a control. CD8⁺ purified T cells were retrovirally transduced, sorted by flow cytometry (GFP-expressing cells) and stimulated with anti-CD3 to analyze their proliferation and capacity to produce IL-2. Two sgRNAs were tested for their cleavage efficacy. An average of $49.1 \pm 7.81\%$ and $5.3 \pm 2.3\%$ of indels were obtained for sg1-FOXP3 and sg2-FOXP3 respectively, and thus sg1 was selected. CD8⁺ T cells transduced with the RV encoding sg1-FOXP3 (CD8-sg1FOXP3) proliferated significantly more and produced higher amounts of IL-2 after α CD3 stimulation than CD8⁺ T cells transduced with the control RV-GFP (CD8-GFP) (Fig. 3e). IFN- γ production after PMA/Ionomycin

stimulation was also improved in CD8-sg1FOXP3 (Fig. 3f) suggesting that FOXP3 silencing improves CD8⁺ T cell functionality in response to stimulation.

To better determine whether FOXP3 alters CD8⁺ T cell function, we also generated several mixed bone marrow chimeric mice. B6Cg-FOXP3^{sf}/J(Scurfy) mice harbor a spontaneous mutation in the FOXP3 gene which impairs Treg activity and leads to the development of an X-linked lymphoproliferative disease characterized by several clinical disorders with marked splenomegaly and enlarged lymph nodes [30] (Suppl Fig. 6a and 6c). FOXP3^{sf} males generally die by 16–25 days of

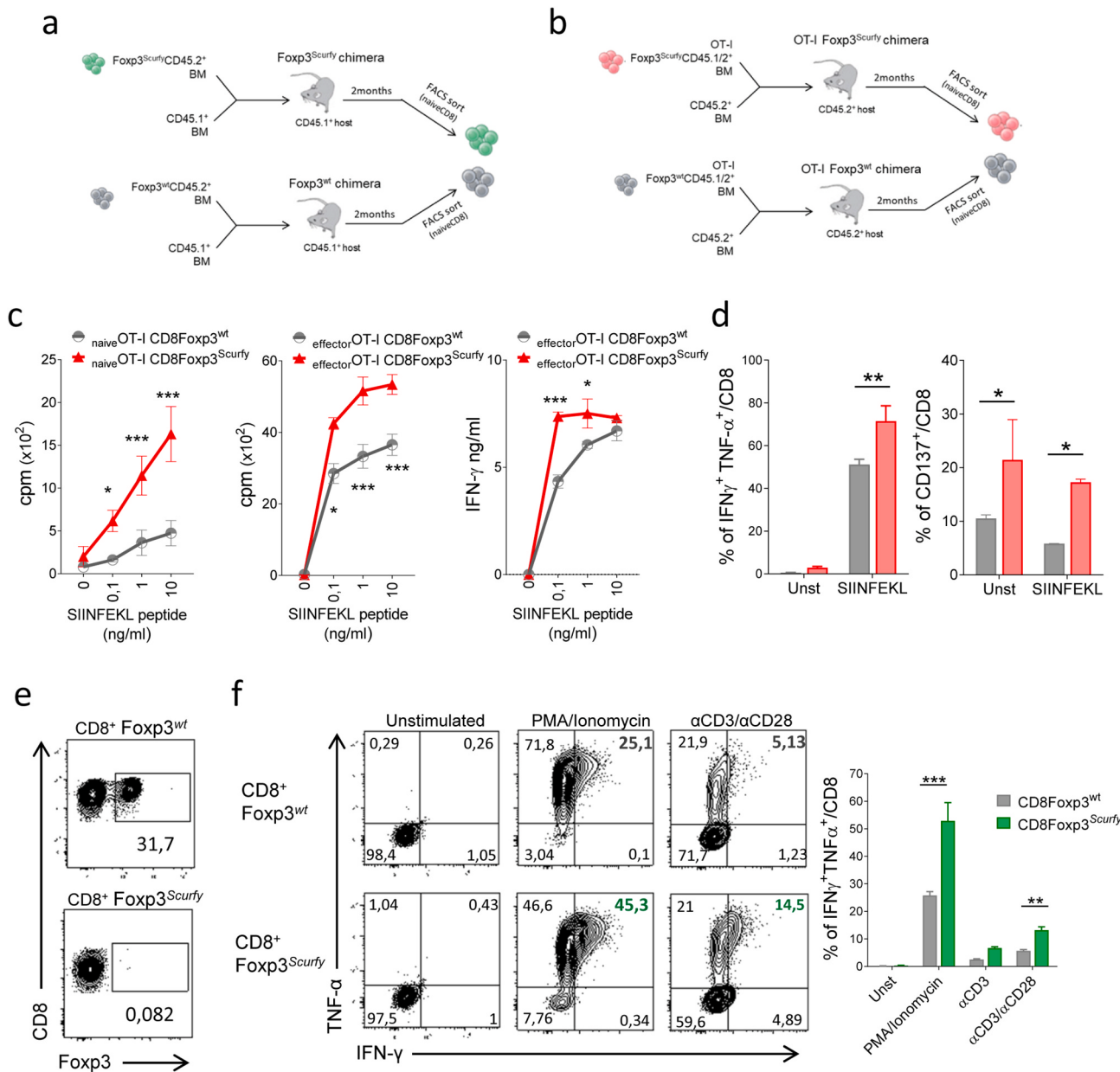


Fig. 4. FOXP3 silencing in CD8⁺ T cells enhances their function in response to TCR stimulation *in vitro* **(a–b)** Mice were reconstituted with mixtures of congenically distinct Foxp3^{wt} and Foxp3^{Scurfy} bone marrow cells (BM), for a wild type TCR repertoire model **(a)** or for OT-1 TCR-transgenic CD8 T cells **(b)**. **(c–d)** Congenically distinct naïve or effector CD8Foxp3^{wt} and CD8Foxp3^{Scurfy} CD45.1/2⁺ OT-1 TCR-transgenic CD8⁺ T cells were sorted from chimeric mice. **(c)** FACS-sorted CD8 cells were stimulated with SIINFEKL peptide at a dose curve ranging from 10 to 0.1 ng/ml to analyze their proliferation rate and IFN- γ production levels using ELISA. **(d)** TNF- α IFN- γ positive cells after brief stimulation *ex vivo* with SIINFEKL peptide (**left**) and CD137⁺ cells (**right**). **(e–f)** Congenically distinct naïve Foxp3^{wt} and Foxp3^{Scurfy} CD45.2+ CD8⁺ T cells were sorted from chimeric mice. **(e)** Flow cytometry for FOXP3 expression after 5 days of culture in the presence of α CD3/CD28 coated antibody plates plus TGF- β (5 ng/ml). **(f)** Flow cytometry exemplifying intracellular cytokine staining for TNF- α and IFN- γ after brief stimulation *ex vivo* with PMA/Ionomycin or α CD3/ α CD28 coated antibody and frequencies of double-positive cells (**right**). Data are representative of two independently repeated experiments ($n = 3–4$). Numbers in gates indicate percentages. * $p < 0.05$, ** $p < 0.01$, *** $p < 0.005$. Two-way ANOVA with the Bonferroni multiple comparisons test **(c, d, f)**. Bars and error represent the mean and the SEM.

age. Phenotypically, CD4⁺ and CD8⁺ T cells from scurfy mice present an activated status (CD44⁺CD62L⁻) (Suppl Fig. 6e and 6g). Male F1 progeny of heterozygous FOXP3^{sf/+} females and male OT-1 transgenic mice are viable and show no apparent external phenotype at day 21 after birth (Suppl Fig. 6b and 6d). However, they presented splenomegaly and lymphadenomegaly and their CD4⁺ and CD8⁺ showed an activated status (CD44⁺CD62L⁻) (*Supplementary Figs. 6f and 6h*). CD4⁺ and CD8⁺ T cells that have undergone thymic positive selection expressing OT-1 α/β chains mis-paired with endogenous TCR β/α chains, respectively, exist in such animals preventing the conclusion that the inflammation caused is due to an intrinsic effect of FOXP3 on CD8⁺ T cells.

To evaluate the cell-intrinsic effect of the absence of FOXP3 on CD8⁺ T cells, we generated different bone marrow chimeras to allow for the presence of FOXP3-deficient CD8⁺ T cells in the absence of the inflammatory background associated with overall FOXP3-deficiency. Irradiated C57BL/6 CD45.1 mice were reconstituted with bone marrow cells from CD45.2⁺ Foxp3^{Scurfy} or from CD45.2⁺ Foxp3^{wt} littermate mice mixed with bone marrow cells from CD45.1⁺ wild type mice (to generate Foxp3^{Scurfy} or Foxp3^{wt} chimeras). In addition, we generated the OT-1 specific chimeras OT-1 Foxp3^{Scurfy} and OT-1 Foxp3^{wt} by reconstituting the bone marrow of irradiated C57BL/6 CD45.2⁺ mice with equal mixtures of bone marrow cells from CD45.1^{+/2+} OT-1 Foxp3^{Scurfy} mice or from CD45.1^{+/2+} OT-1 Foxp3^{wt} litter mice, with bone marrow cells from CD45.2⁺ wild type mice (See diagrams of the strategy in *Fig. 4a–b*, respectively). Two months after reconstitution, we found that Foxp3^{Scurfy} chimeric mice had lower engraftment of CD45.2⁺ scurfy cells (with a CD45.2/CD45.1 ratio below 0.2 as compared with the engraftment of CD45.2 wt cells (Suppl Fig. 7c and 7e). Interestingly, no significant changes in the number of naïve CD8 (CD44⁻CD62L⁺) or memory CD8⁺ (CD44⁺CD62L⁺) T cells, were observed between both chimeras. Only a slight increase in the percentage of effector CD8⁺ (CD44⁺CD62L⁻) T cells was observed in the lymph nodes of Foxp3^{Scurfy} chimeric mice (Suppl Figure 7f-right). In the case of OT-1 Foxp3^{Scurfy} and OT-1 Foxp3^{wt} chimeras, the reconstitution levels were very similar between both chimeras, with no significant changes in the number of naïve, effector or memory CD8 T cells (Suppl Fig. 7d, 7g and 7h) suggesting no differences in the steady state of lymphocyte development. Importantly, these results also indicate that the absence of FOXP3 on CD8 cells does not in itself drive inflammation. We used CD8⁺ T cells from these chimeras to determine the cell-intrinsic function of FOXP3 in regulating CD8⁺ T cell activity *in vitro* and *in vivo*. We found that naïve OT-1 Foxp3^{Scurfy} T cells experienced higher proliferation rates than OT-1 Foxp3^{wt} T cells in response to increasing concentrations of the SIINFEKL peptide (from 0.1 to 10 ng/ml). This improved proliferative capacity was also observed in effector OT-1 Foxp3^{Scurfy} T cells, which was accompanied by higher IFN- γ production (*Fig. 4c*). Moreover, the percentage of CD137⁺ cells or IFN- γ /TNF- α double positive T cells was significantly increased in response to SIINFEKL stimulation in effector OT-1 Foxp3^{Scurfy} T cells as compared to OT-1 Foxp3^{wt} T cells (*Fig. 4d*).

The lack of FOXP3 expression in these mice chimeras was confirmed when CD8⁺ T cells from Foxp3^{Scurfy} or Foxp3^{wt} chimeric mice were stimulated *in vitro* with α CD3 and α CD28 antibodies in the presence of IL-2 and TGF- β . Indeed, while 30% of CD8⁺ T cells from Foxp3^{wt} chimeric mice upregulated FOXP3 under these culture conditions, no FOXP3⁺ T cells were detected in CD8⁺ T cells from Foxp3^{Scurfy} mice (*Fig. 4e*). Importantly, when CD8⁺ T cells cultured in the presence of iTreg polarizing conditions were stimulated with PMA/Ionomycin or with α CD3/CD28 beads, we found a significantly higher percentage of IFN- γ ⁺/TNF- α ⁺ cells in the CD8⁺ T cells from Foxp3^{Scurfy} chimeric mice as compared to CD8⁺ T cells from Foxp3^{wt} chimeric mice (*Fig. 4f*).

3.6. FOXP3-deficient CD8⁺ T cells exhibit normal memory T cell differentiation

The differentiation process, from naïve to effector, to terminally differentiated effector or memory T cells is thought to be orchestrated by

a network of transcription factors [31,32]. To evaluate if silencing FOXP3 has an impact on this differentiation process, naïve CD8⁺ T cells obtained from the OT-1 Foxp3^{Scurfy} and OT-1 Foxp3^{wt} chimeras were adoptively transferred into CD45.2 mice. Four hours after T cell transfer, mice were immunized with ovalbumin plus Poly I:C to induce activation of OT-1 T cells. Five days later, mice were bled to measure the activation status of the OT-1 transferred cells (d5 effector T cells). Mice received a boosting immunization at day 45 and were sacrificed at day 55 to measure the induction of a long-lived memory response (*Fig. 5a*). Analysis of blood samples five days after *in vivo* priming showed a significantly higher expansion of OT-1 T cells in mice receiving OT-1 Foxp3^{Scurfy} T cells as compared mice receiving OT-1 Foxp3^{wt} T cells (*Fig. 5b–c*). Phenotypically, no significant changes were observed in the level of expression of CD44, CD25 or CD69 in the transferred cells, although OT-1 Foxp3^{Scurfy} T cells had a higher percentage of effector CD44⁺CD62L⁻ cells (Suppl Figure 8a). The differences in the expansion capacity of transferred OT-1 T cells were not observed at day 49 and 55 (ten days after the ovalbumin boost). There were no significant changes in the percentage of OT-1 T cells in the blood or spleen of mice receiving either OT-1 Foxp3^{Scurfy} or OT-1 Foxp3^{wt} naïve T cells (*Fig. 5d* and Suppl Figure 8c). Similarly, no changes in the percentage of naïve, effector or memory T cells were observed (*Supplementary Fig. 8b*). However, OT-1 T cells from mice receiving OT-1 Foxp3^{Scurfy} T cells were able to mount a stronger response to stimulation with the SIINFEKL peptide or to PMA/Ionomycin (measured by flow cytometry as percentage of IFN- γ /TNF- α producing CD8 T cells or by ELISPOT as the number of IFN- γ producing splenocytes) (*Fig. 5e* and Suppl Figure 8d, respectively) suggesting that lack of FOXP3 does not impair the differentiation of naïve CD8⁺ T cells into memory cells but rather improved it.

3.7. FOXP3-deficient CD8⁺ T cells exhibit an improved antitumor immune response

We then evaluated the impact of FOXP3 deficiency on the anti-tumor activity of CD8⁺ T cells. C57BL/6 mice bearing B16-OVA tumors were treated i.v. with 1.2×10^6 naïve OT-1 Foxp3^{Scurfy} or naïve OT-1 Foxp3^{wt} T cells obtained from the corresponding bone marrow chimeric mice (*Fig. 6a*). Adoptive transfer of OT-1 T cells delayed tumor growth. Notably, this delay was significantly longer in mice receiving OT-1 Foxp3^{Scurfy} T cells than in mice transferred with OT-1 Foxp3^{wt} T cells and these mice also showed longer overall survival (*Fig. 6b*). Indeed, 33% of the animals receiving OT-1 Foxp3^{Scurfy} T cells were able to reject the tumor, whereas none of the animals receiving OT-1 Foxp3^{wt} T cells did.

In order to evaluate the phenotype and function of the CD8⁺ T cells *in vivo*, we carried out parallel experiments with a reduced number of animals ($n = 3$ mice per group) that were sacrificed seven days after T cell infusion to characterize the phenotype of the transferred lymphocytes. It was found that mice that received OT-1 Foxp3^{Scurfy} T cells exhibited a significant trend toward having a higher number of IFN- γ producing cells in response to the SIINFEKL peptide (measured by ELISPOT) in the spleen than mice transferred with OT-1 Foxp3^{wt} T cells (*Fig. 6c*). Similarly, mice that received OT-1 Foxp3^{Scurfy} T cells had a higher percentage of activated OT-1 cells (CD44⁺) that produced more IFN- γ in the tumor draining lymph nodes (as measured by flow cytometry) (*Fig. 6d*). Notably, mice receiving OT-1 Foxp3^{Scurfy} T cells had higher numbers of tumor infiltrating OT-1 T cells, with a higher percentage of IFN- γ /TNF- α producing cells and higher KI-67 proliferation marker, but with a lower percentage of LAG3⁺ cells, than mice transferred with OT-1 Foxp3^{wt} T cells (*Fig. 6e*).

3.8. Transcriptomic changes in FOXP3-deficient CD8⁺ T cells

In order to better characterize the functional differences observed by the absence of FOXP3 in CD8⁺ T lymphocytes, we performed a transcriptomic analysis using MARSSec technology. Highly purified OT-1

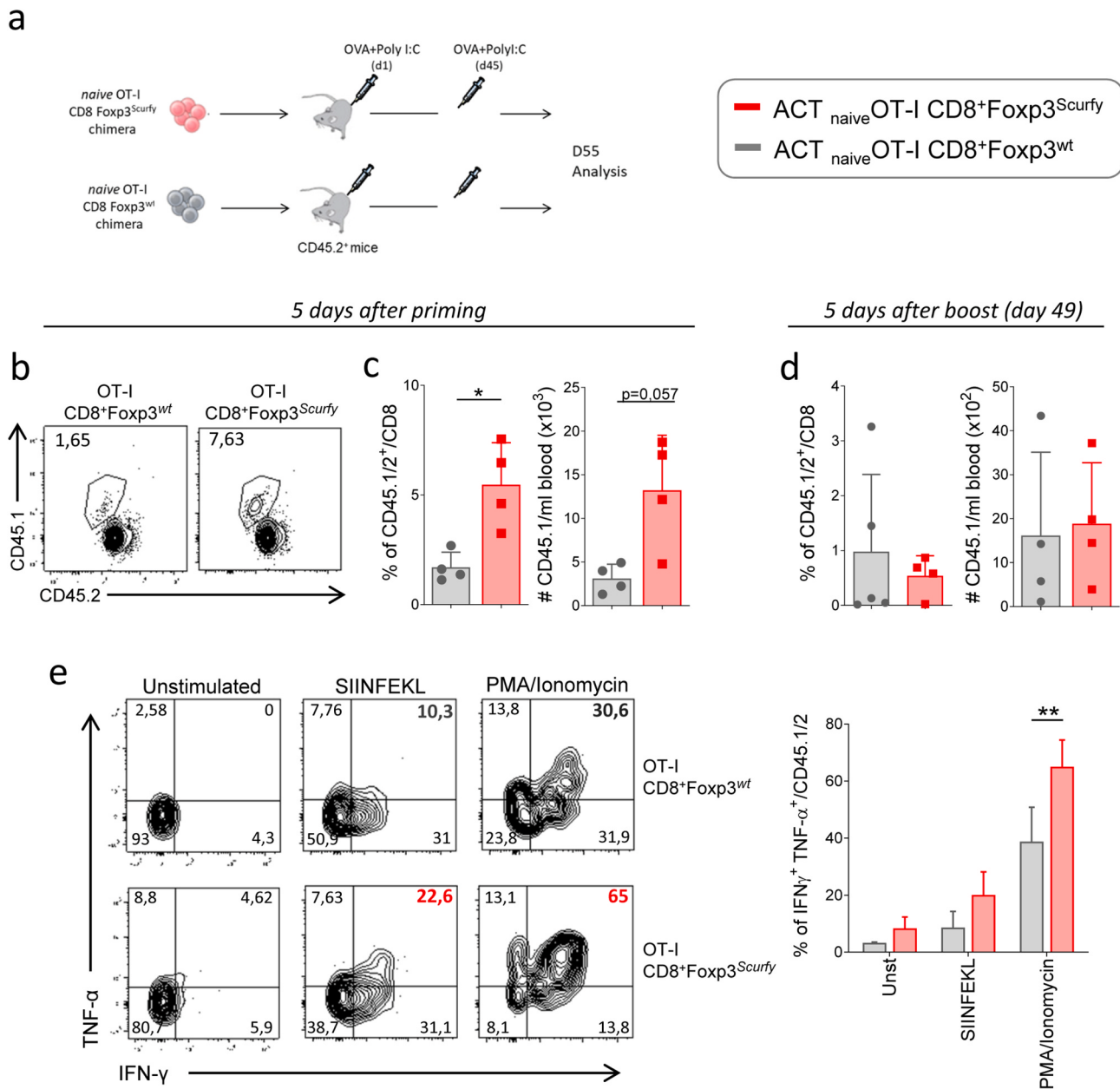


Fig. 5. FOXP3 silencing does not impair memory OT-I CD8 T-cell generation. (a) Experimental design assessing FOXP3 function in long-term memory in CD8 T cells. Naive CD8⁺ OT-I Foxp3^{Scurfy} or OT-I Foxp3^{WT} T cells (5×10^5 cells/mouse, CD451/2⁺ T phenotype) were transferred into CD45.2⁺ mice which were vaccinated intravenously with OVA protein (45 µg/mouse) and PolyI:C (50 µg/mouse) at day 1 and 45 after T cell infusion (n = 4 mice per group per time point). (b) Flow cytometry exemplifying CD451/2⁺ T cell frequencies in blood, 5 days after transfer. (c) Percentage (left) and total numbers per ml (right) of CD45.1/2⁺/CD8 T cells, 5d after vaccination. (d) Percentage (left) and total numbers per ml of blood (right) of CD45.1/2⁺/CD8 T cells at day 5 after second dose of vaccine (day 49 after cell transfer). (e) Intracellular cytokine staining (TNF- α and IFN- γ) of splenic transferred T cells and percentage of double positive cells after brief stimulation with the SIINFEKL peptide (1 µg/ml) or PMA/Ionomycin ex vivo at day 55 after T cell transfer. Data are shown after gating on live CD45.1/2⁺CD8⁺ cells. Data are representative of two independently repeated experiments (n = 4). Numbers in gates indicate percentages. *p < 0,05, **p < 0,01, ***p < 0,005. Student t-test (c), Two-way ANOVA with the Bonferroni multiple comparisons test (e, f). Bars and error represent the mean and the SEM.

Foxp3^{Scurfy} and OT-I Foxp3^{WT} T cells from the corresponding BM chimeric mice were isolated and stimulated with 1 ng/ml of SIINFEKL peptide for 6 h in culture medium. RNA was then isolated and sequenced for the analysis of differential expression of mRNA transcripts. First principal components (PC1) analyses accounted for 96% of the variance between T cells stimulated with the SIINFEKL peptide and unstimulated cells (Fig. 7a). We focused on the comparisons after TCR stimulation with SIINFEKL, which was shown to induce FOXP3 on T cells. Considering those genes with a fold change >1, 55 genes were upregulated and 17 downregulated in OT-I Foxp3^{Scurfy} T cells (p < 0.05) with respect to Foxp3^{WT} T cells (represented in the volcano and heatmap plots in Fig. 7b

and c respectively). Gene set enrichment analysis comparing OT-I Foxp3^{Scurfy} T cells with OT-I Foxp3^{WT} T cells after stimulation with the peptide revealed a significant enrichment of genes implicated in the response to IFN- γ , IFN- α , inflammatory response, IL-6/JAK/STAT, G2M checkpoint and IL-2/STAT signaling (Fig. 7d).

Raw data and normalized dataframes from this experiment are available from the Gene Expression Omnibus (GEO) at GSE181510.

4. Discussion

This study was conducted to gain an understanding of the role of the

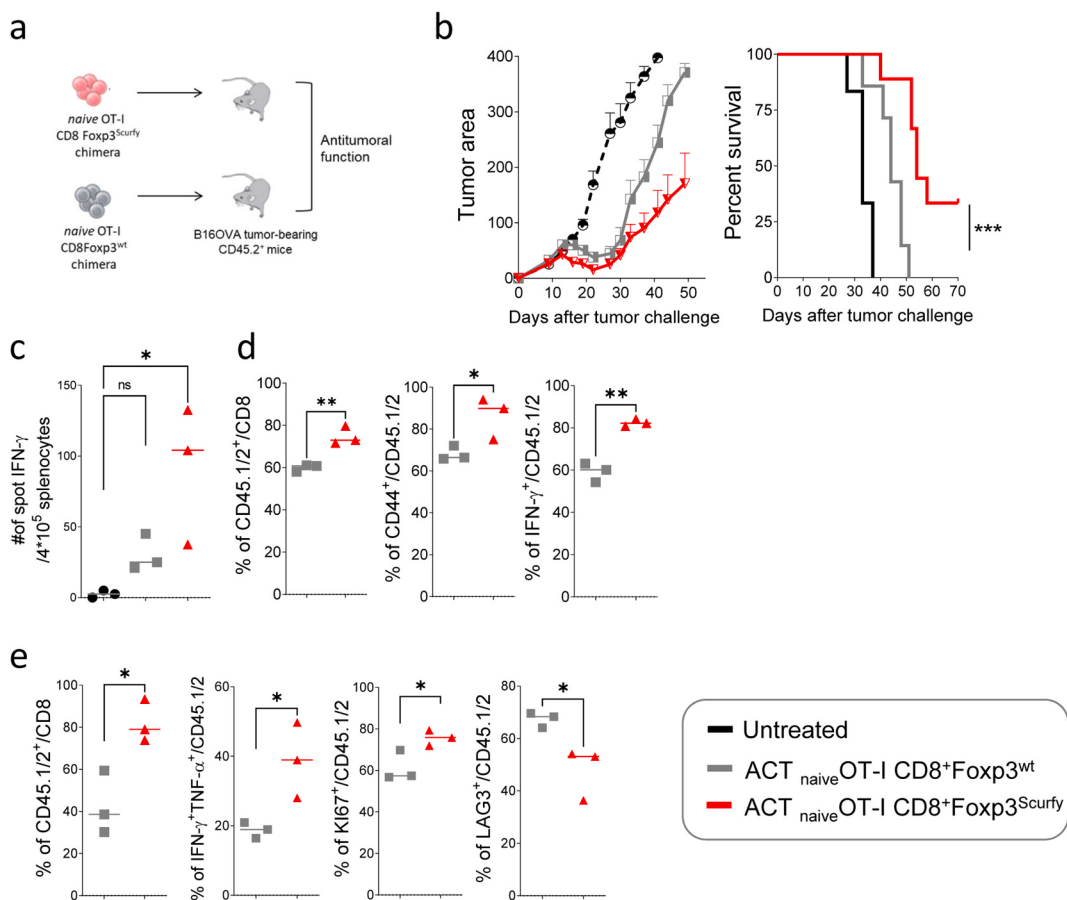


Fig. 6. Adoptive cell transfer of naïve CD8 OT-1 Foxp3^{Scurfy} T cells show improved antitumor efficacy. (a) Experimental design: 1.2×10^6 naïve CD8⁺ OT-1 Foxp3^{Scurfy} or OT-1 Foxp3^{wt} T cells were adoptively transferred into B16-OVA-bearing CD45.2+ mice. (n = 8 mice per group). (b) B16-OVA tumor growth at different time points following tumor challenge (left) and Kaplan-Meier plots of mouse survival (right) (n = 7–8 mice per group). (c, d) Percentages, phenotypic and functional analysis of CD45.1/2⁺CD8⁺ T cells 7 days after their adoptive T cell transfer, in the spleen (c) and the tumor draining lymph nodes (d) and within the tumor (e). (n = 3). Data are shown after gating on live CD45⁺CD8⁺ cells. Data are representative of two independently repeated experiments. *p < 0.05, **p < 0.01, ***p < 0.005. (a), Log rank test (b), Student ttest (c, d, e). Bars and error represent the mean and the SEM.

expression of FOXP3 in CD8⁺ T cell function after TCR stimulation. It was suggested that tumor cells may act as tolerogenic antigen-presenting cells and induce FOXP3 expression in both CD4⁺ and CD8⁺ T cells, suppressing the anti-tumor immune response [33,34]. In the setting of adoptive cell therapies against cancer, it was also reported that tumor-specific CD8⁺ T cells transferred into tumor-bearing mice traffic to the tumor tissue where they might be induced to become CD8⁺ suppressor cells [15,35]. However, the potential role of FOXP3 in this process was not clearly demonstrated.

As occurred in CD4⁺ T cells [36], we found that ectopic expression of FOXP3 in CD8⁺ T cells via RV transduction reduced their functionality *in vitro*. In contrast, FOXP3 silencing on CD8⁺ T cells using CRISPR-Cas9 genome editing significantly improved CD8⁺ T cell proliferation and IL-2 and IFN-γ secretion in response to TCR stimulation. Notably, as was described for CD4⁺ T cells [37,38], we found that murine and human CD8⁺ T cells upregulate FOXP3 after suboptimal TCR stimulation *in vitro*, suggesting that the strength of TCR stimulation may modulate CD8⁺ T cell functionality through FOXP3. ERK inhibition reversed the TCR-induced Foxp3 expression suggesting that TCR signaling, despite not being optimal, must be sufficiently strong to activate ERK, at least transiently. ERK signaling and its duration seems to be dependent on TCR strength [39]. In this regard, it has been shown that sustained or transient ERK activation have divergent transcriptional effects [40]. It therefore remains possible that different ERK targets in T cells are differentially affected by the strength of TCR stimulation, which warrants further investigation of the additional downstream components

that may affect Foxp3 expression in CD8 T cells.

The presence of CD8⁺FOXP3⁺ T cells infiltrating tumors [34,41,42] suggests that the tumor microenvironment favors the recruitment of natural CD8⁺FOXP3⁺ T cells or their conversion from conventional antitumor CD8⁺ T cells [15]. In our murine models, we found significant numbers of CD137⁺CD8⁺FOXP3⁺ T cells infiltrating the tumor and the tumor draining lymph nodes. Our adoptive T cell transfer experiments in mice bearing B16-OVA tumors showed that a significant proportion of OT-1 CD8⁺ T cells are converted into CD8⁺FOXP3⁺ overexpressing of CTLA-4, LAG-3 and IL-10 within the tumor. These data suggest that the TCR-induced FOXP3 is taking place within the tumor, impairing CD8⁺ T cell function.

To better study the effect of FOXP3 on antigen-specific CD8⁺ T cells, we generated the OT-1-specific BM chimeric mice OT-1 Foxp3^{Scurfy} and OT-1 Foxp3^{wt}. Using the CD8⁺ T cells from these chimeric mice, we demonstrated that lack of FOXP3 on CD8⁺ T cells conferred a higher proliferative capacity and IFN-γ production in response to low doses of SIINFEKL peptide. These results were confirmed in the transcriptomic analysis when comparing T cells after suboptimal TCR stimulation with SIINFEKL peptide. Indeed, a significant enrichment of genes implicated in response to IFN-gamma, IFN-alpha, inflammatory response, IL-6/JAK/STAT, G2M checkpoint and IL-2/STAT signaling among others were found in OT-1 Foxp3^{Scurfy} with respect to OT-1 Foxp3^{wt} T cells.

FOXP3 can regulate the expression of a number of genes through the formation of a cooperative complex with NFAT [21]. We have found that inhibition of this protein-protein interaction by a short peptide

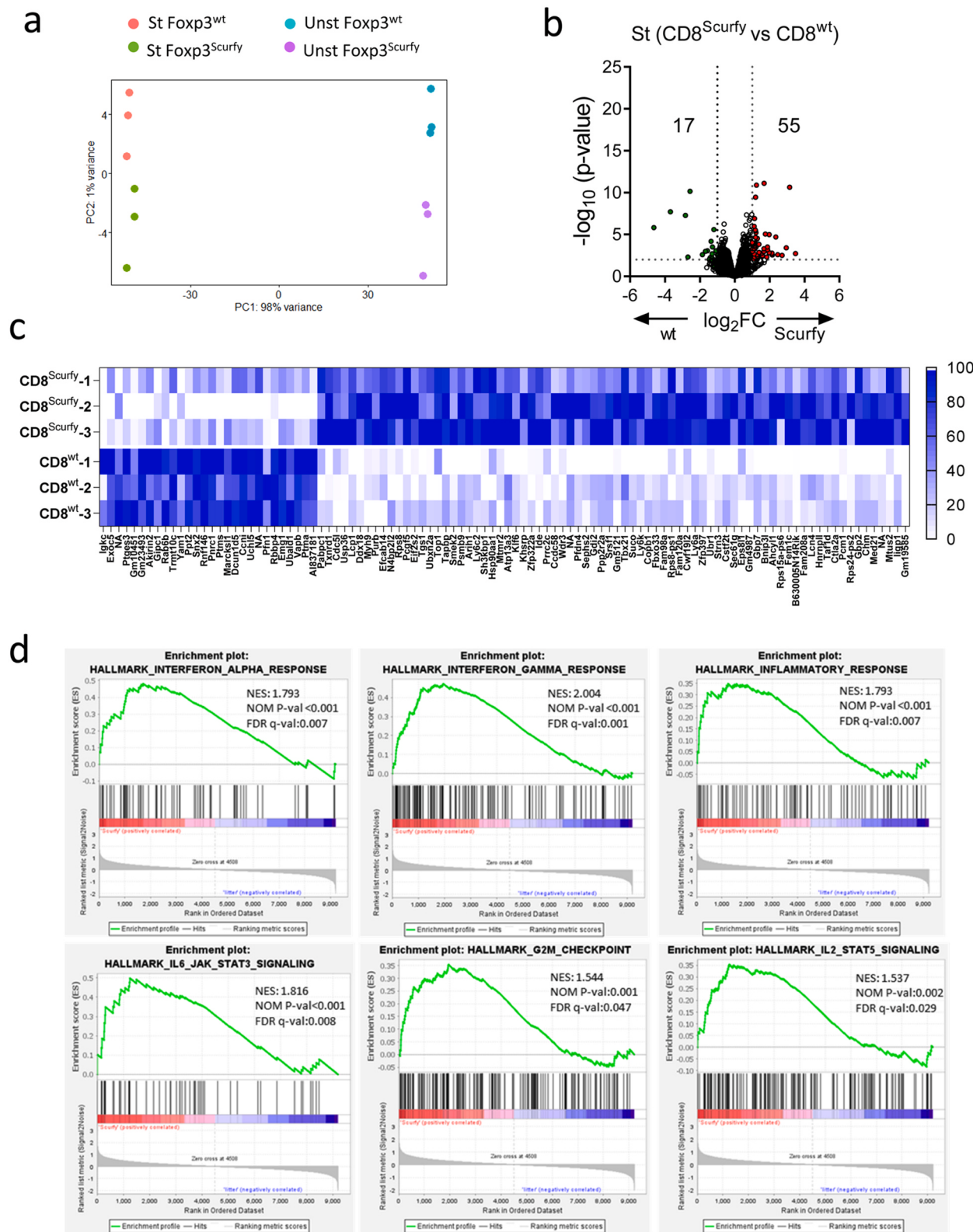


Fig. 7. Transcriptomic analysis of CD8 OT-1 Foxp3^{Scurfy} vs CD8 OT-1 Foxp3^{WT} T cells. Highly purified CD8⁺ OT-1 Foxp3^{Scurfy} and OT-1 Foxp3^{WT} T cells were left unstimulated or stimulated with SIINFEKL peptide for 6 h before transcriptomic analysis. (a) Unsupervised Principal component analysis (PCA) of RNAseq data for all samples used in this study. (b) Volcano plots for differential gene expression of OT-1 Foxp3^{WT} vs OT-1 Foxp3^{Scurfy} stimulated with SIINFEKL peptide (1 ng/ml). Genes with log fold change of ± 1.5 and $p < 0.05$ were considered differentially expressed. Red dots represent upregulated genes in CD8⁺ OT-1 Foxp3^{Scurfy} and green dots represent upregulated genes in CD8⁺ OT-1 Foxp3^{WT}. (c) Gene set enrichment analysis of RNA-Seq data of CD8⁺ OT-1 Foxp3^{WT} and OT-1 Foxp3^{Scurfy} T cells after stimulation with SIINFEKL peptide. FDR q values were calculated using GSEA software. Unst Foxp3^{WT}: unstimulated OT-I CD8Foxp3^{WT}, St Foxp3^{WT}: stimulated OT-I CD8Foxp3^{WT}, Unst Foxp3^{Scurfy}: unstimulated OT-I CD8Foxp3^{Scurfy}, St Foxp3^{Scurfy}: stimulated OT-I CD8Foxp3^{Scurfy}.

improved the proliferation and effector functions of CD8⁺ T cells in response to TCR stimulation, suggesting that FOXP3/NFAT interaction plays a role in the regulatory function of FOXP3 also in CD8⁺ T cells.

Several transcription factors regulate effector and memory CD8⁺ T cell development (reviewed in Ref. [43]). It could be hypothesized that the absence of FOXP3 on CD8⁺ T cells favors the acquisition of a more effector phenotype that might impair their long-term fate in terms of their ability to populate the memory T cell pool *in vivo*. However, our prime/boost experiments with adoptively transferred CD8⁺ T cells suggest that this is not the case. As expected, mice receiving OT-1 Foxp3^{Scurfy} T cells and immunized with OVA five days after transfer, had a higher proliferation of CD8⁺ OT-1 T cells in response to *in vivo* priming with the OVA protein. These differences in the proliferative capacity of transferred CD8 OT-1 T cells leveled out when mice were boosted at day 49. However, OT-1 Foxp3^{Scurfy} T cells still maintained a higher functionality in terms of IFN-γ and TNF-α production suggesting that the lack of FOXP3 is not detrimental to the regulation of CD8⁺ T cell memory development.

Importantly, we found that CD8⁺ T cells lacking FOXP3 exhibited an enhanced therapeutic effect *in vivo* in tumor-bearing mice. Adoptive transfer of OT-1 Foxp3^{Scurfy} T cells in C57BL/6 mice bearing B16-OVA tumors significantly delayed tumor growth as compared to mice receiving OT-1 Foxp3^{WT} T cells with 33% of mice rejecting the tumors completely. This is particularly relevant in a model in which adoptive T cell transfer experiments are not very efficient because OVA antigen expression is rapidly lost in B16-OVA cells due to immune pressure [44, 45]. As was suggested to occur in adoptively transferred CD4⁺ T cells [46], our results suggest that FOXP3 expression on CD8⁺ T cells is an early and tumor-related event that may limit anti-tumor efficacy.

In summary, our data suggest that FOXP3 expression in CD8⁺ T cells could act as a feedback mechanism to quickly turn off the activation status of the effector T cells infiltrating the tumor and contribute to the loss of antitumor responses of adoptively transferred T cells. Strategies aimed at inhibiting FOXP3 can act, not only on Treg cells and conventional CD4⁺ T cells, but also on CD8 T cells after suboptimal TCR stimulation, constituting a more attractive target for the development of new therapies against cancer.

Funding

The work was supported by grants from Ministerio de Educación y Ciencia (SAF2010-15060 and SAF2013-42772-R to J.J.L.), Ministerio de Ciencia e Innovación (PID2019-108989RB-I00, PLEC2021-008094 MCIN/AEI/10.13039/501100011033, AUTOCART, RTC-2017-6585-1) and the European Union (CARAMBA, SC1-PM-08-2017. Contract 754658), Gobierno de Navarra (0011-1411-2019-000079; Proyecto DESCARTHeS), Fundación Ramón Areces (to E.C., S.H.S. and J.J.L.) and Paula & Rodger Riney Foundation. TL is recipient of a Juan de la Cierva grant (IJC-2017-34204).

Authors' contributions

Conceptualization, T.L., S.H-S, R.R. and J.J.L.; Methodology, T.L., E. C., D.A., J.P.R., A.V., N.C. and J.J.L.; Investigation, T.L., E.C., C.M.O., F. N., A.L-C., R.N., D.A., M.G., A.V., N.C. and J.J.L.; Writing –Original Draft, T.L and J.J.L.; Writing –Review & Editing, T.L., F.N., P.S., R.R., S. H-S., N.C. and J.J.L.; Funding Acquisition, T.L., R.R. and J.J.L.; Resources, J.P.R.; Supervision, T.L. and J.J.L.

Data availability

The data generated in this study are available within the article and its supplementary data files. The expression profile data analyzed in this study are available from Gene Expression Omnibus (GEO) at GSE181510.

Declaration of competing interest

The authors declare that they have no known competing financial interests or personal relationships that could have appeared to influence the work reported in this paper.

Acknowledgements

We thank Elena Ciordia and Eneko Elizalde for excellent animal care and the Blood Bank of Navarra (Biobanco, IDISNA) for their collaboration. We also thank Ibon Tamayo for his assistance in the microarray experiments.

Appendix A. Supplementary data

Supplementary data to this article can be found online at <https://doi.org/10.1016/j.canlet.2021.12.030>.

References

- [1] S.A. Rosenberg, N.P. Restifo, Adoptive cell transfer as personalized immunotherapy for human cancer, *Science* 348 (6230) (2015) 62–68.
- [2] J. Crespo, H. Sun, T.H. Welling, Z. Tian, W. Zou, T cell anergy, exhaustion, senescence, and stemness in the tumor microenvironment, *Curr. Opin. Immunol.* 25 (2) (2013) 214–221.
- [3] W. Seo, C. Jerin, H. Nishikawa, Transcriptional regulatory network for the establishment of CD8(+) T cell exhaustion, *Exp. Mol. Med.* 53 (2) (2021) 202–209.
- [4] I. Apostolou, A. Saruhan, L. Klein, H. von Boehmer, Origin of regulatory T cells with known specificity for antigen, *Nat. Immunol.* 3 (8) (2002) 756–763.
- [5] M.S. Jordan, A. Boesneau, A.J. Reed, A.L. Petrone, A.E. Holenbeck, M.A. Lerman, et al., Thymic selection of CD4+CD25+ regulatory T cells induced by an agonist self-peptide, *Nat. Immunol.* 2 (4) (2001) 301–306.
- [6] W. Chen, W. Jin, N. Hardegen, K.J. Lei, L. Li, N. Marinos, et al., Conversion of peripheral CD4+CD25- naive T cells to CD4+CD25+ regulatory T cells by TGF-β beta induction of transcription factor Foxp3, *J. Exp. Med.* 198 (12) (2003) 1875–1886.
- [7] S. Liang, P. Alard, Y. Zhao, S. Parnell, S.L. Clark, M.M. Kosiewicz, Conversion of CD4+ CD25- cells into CD4+ CD25+ regulatory T cells in vivo requires B7 costimulation, but not the thymus, *J. Exp. Med.* 201 (1) (2005) 127–137.
- [8] J. Wang, A. Ioan-Facsinay, E.I. van der Voort, T.W. Huizinga, R.E. Toes, Transient expression of FOXP3 in human activated nonregulatory CD4+ T cells, *Eur. J. Immunol.* 37 (1) (2007) 129–138.
- [9] B. Valzasina, S. Picone, C. Guiducci, M.P. Colombo, Tumor-induced expansion of regulatory T cells by conversion of CD4+CD25- lymphocytes is thymus and proliferation independent, *Cancer Res.* 66 (8) (2006) 4488–4495.
- [10] T. Lozano, L. Villanueva, M. Durantez, M. Gorraiz, M. Ruiz, V. Belsue, et al., Inhibition of FOXP3/NFAT interaction enhances T cell function after TCR stimulation, *J. Immunol.* 195 (7) (2015) 3180–3189.
- [11] B. Bisikirska, J. Colgan, J. Luban, J.A. Bluestone, K.C. Herold, TCR stimulation with modified anti-CD3 mAb expands CD8+ T cell population and induces CD8+CD25+ Tregs, *J. Clin. Invest.* 115 (10) (2005) 2904–2913.
- [12] M.E. Morgan, J.H. van Bilsen, A.M. Bakker, B. Heemskerk, M.W. Schilham, F. C. Hartgers, et al., Expression of FOXP3 mRNA is not confined to CD4+CD25+ T regulatory cells in humans, *Hum. Immunol.* 66 (1) (2005) 13–20.
- [13] V. Pillai, S.B. Ortega, C.K. Wang, N.J. Karandikar, Transient regulatory T-cells: a state attained by all activated human T-cells, *Clin. Immunol.* 123 (1) (2007) 18–29.
- [14] C.T. Mayer, S. Floess, A.M. Baru, K. Lahl, J. Huehn, T. Sparwasser, CD8+ Foxp3+ T cells share developmental and phenotypic features with classical CD4+ Foxp3+ regulatory T cells but lack potent suppressive activity, *Eur. J. Immunol.* 41 (3) (2011) 716–725.
- [15] K.A. Shafer-Weaver, M.J. Anderson, K. Stagliano, A. Malyguine, N.M. Greenberg, A.A. Hurwitz, Cutting Edge: tumor-specific CD8+ T cells infiltrating prostatic tumors are induced to become suppressor cells, *J. Immunol.* 183 (8) (2009) 4848–4852.
- [16] L. Chen, J.N. Glover, P.G. Hogan, A. Rao, S.C. Harrison, Structure of the DNA-binding domains from NFAT, Fos and Jun bound specifically to DNA, *Nature* 392 (6671) (1998) 42–48.
- [17] F. Macian, F. Garcia-Cozar, S.H. Im, H.F. Horton, M.C. Byrne, A. Rao, Transcriptional mechanisms underlying lymphocyte tolerance, *Cell* 109 (6) (2002) 719–731.
- [18] T. Fehr, C.L. Lucas, J. Kurtz, T. Onoe, G. Zhao, T. Hogan, et al., A CD8 T cell-intrinsic role for the calcineurin-NFAT pathway for tolerance induction *in vivo*, *Blood* 115 (6) (2010) 1280–1287.
- [19] G.J. Martinez, R.M. Pereira, T. Aijo, E.Y. Kim, F. Marangoni, M.E. Pipkin, et al., The transcription factor NFAT promotes exhaustion of activated CD8(+) T cells, *Immunity* 42 (2) (2015) 265–278.
- [20] H.S. Bandukwala, Y. Wu, M. Feuerer, Y. Chen, B. Barboza, S. Ghosh, et al., Structure of a domain-swapped FOXP3 dimer on DNA and its function in regulatory T cells, *Immunity* 34 (4) (2011) 479–491.

- [21] Y. Wu, M. Borde, V. Heissmeyer, M. Feuerer, A.D. Lapan, J.C. Stroud, et al., FOXP3 controls regulatory T cell function through cooperation with NFAT, *Cell* 126 (2) (2006) 375–387.
- [22] E. Bettelli, M. Dastrange, M. Oukka, Foxp3 interacts with nuclear factor of activated T cells and NF-kappa B to repress cytokine gene expression and effector functions of T helper cells, *Proc. Natl. Acad. Sci. U. S. A.* 102 (14) (2005) 5138–5143.
- [23] M. Ono, H. Yaguchi, N. Ohkura, I. Kitabayashi, Y. Nagamura, T. Nomura, et al., Foxp3 controls regulatory T-cell function by interacting with AML1/Runx1, *Nature* 446 (7136) (2007) 685–689.
- [24] D. Rudra, P. deRoos, A. Chaudhry, R.E. Nicc, A. Arvey, R.M. Samstein, et al., Transcription factor Foxp3 and its protein partners form a complex regulatory network, *Nat. Immunol.* 13 (10) (2012) 1010–1019.
- [25] E.K. Brinkman, T. Chen, M. Amendola, B. van Steensel, Easy quantitative assessment of genome editing by sequence trace decomposition, *Nucleic Acids Res.* 42 (22) (2014) e168.
- [26] S.G. Zheng, J.D. Gray, K. Ohtsuka, S. Yamagiwa, D.A. Horwitz, Generation ex vivo of TGF-beta-producing regulatory T cells from CD4+CD25- precursors, *J. Immunol.* 169 (8) (2002) 4183–4189.
- [27] D.T. Le, B.H. Ladle, T. Lee, V. Weiss, X. Yao, A. Leubner, et al., CD8(+) Foxp3(+) tumor infiltrating lymphocytes accumulate in the context of an effective anti-tumor response, *Int. J. Cancer* 129 (3) (2011) 636–647.
- [28] J.D. Fontenot, M.A. Gavin, A.Y. Rudensky, Foxp3 programs the development and function of CD4+CD25+ regulatory T cells, *Nat. Immunol.* 4 (4) (2003) 330–336.
- [29] Q. Li, A. Shakya, X. Guo, H. Zhang, D. Tantin, P.E. Jensen, et al., Constitutive nuclear localization of NFAT in Foxp3+ regulatory T cells independent of calcineurin activity, *J. Immunol.* 188 (9) (2012) 4268–4277.
- [30] C.L. Bennett, J. Christie, F. Ramsdell, M.E. Brunkow, P.J. Ferguson, L. Whitesell, et al., The immune dysregulation, polyendocrinopathy, enteropathy, X-linked syndrome (IPEX) is caused by mutations of FOXP3, *Nat. Genet.* 27 (1) (2001) 20–21.
- [31] J.A. Best, D.A. Blair, J. Knell, E. Yang, V. Mayya, A. Doedens, et al., Transcriptional insights into the CD8(+) T cell response to infection and memory T cell formation, *Nat. Immunol.* 14 (4) (2013) 404–412.
- [32] S.M. Kaech, S. Hemby, E. Kersh, R. Ahmed, Molecular and functional profiling of memory CD8 T cell differentiation, *Cell* 111 (6) (2002) 837–851.
- [33] M.A. Frassanito, S. Ruggieri, V. Desantis, L. Di Marzo, P. Leone, V. Racanelli, et al., Myeloma cells act as tolerogenic antigen-presenting cells and induce regulatory T cells in vitro, *Eur. J. Haematol.* 95 (1) (2015) 65–74.
- [34] S. Zhang, X. Ke, S. Zeng, M. Wu, J. Lou, L. Wu, et al., Analysis of CD8+ Treg cells in patients with ovarian cancer: a possible mechanism for immune impairment, *Cell. Mol. Immunol.* 12 (5) (2015) 580–591.
- [35] M.J. Anderson, K. Shafer-Weaver, N.M. Greenberg, A.A. Hurwitz, Tolerization of tumor-specific T cells despite efficient initial priming in a primary murine model of prostate cancer, *J. Immunol.* 178 (3) (2007) 1268–1276.
- [36] S. Hori, T. Nomura, S. Sakaguchi, Control of regulatory T cell development by the transcription factor Foxp3, *Science* 299 (5609) (2003) 1057–1061.
- [37] S.P. Cobbold, R. Castejon, E. Adams, D. Zelenika, L. Graca, S. Humm, et al., Induction of foxP3+ regulatory T cells in the periphery of T cell receptor transgenic mice tolerized to transplants, *J. Immunol.* 172 (10) (2004) 6003–6010.
- [38] V.G. Oliveira, M. Caridade, R.S. Paiva, J. Demengeot, L. Graca, Sub-optimal CD4+ T-cell activation triggers autonomous TGF-beta-dependent conversion to Foxp3+ regulatory T cells, *Eur. J. Immunol.* 41 (5) (2011) 1249–1255.
- [39] G. Altan-Bonnet, R.N. Germain, Modeling T cell antigen discrimination based on feedback control of digital ERK responses, *PLoS Biol.* 3 (11) (2005) e356.
- [40] K. Aoki, Y. Kumagai, A. Sakurai, N. Komatsu, Y. Fujita, C. Shionyu, et al., Stochastic ERK activation induced by noise and cell-to-cell propagation regulates cell density-dependent proliferation, *Mol. Cell.* 52 (4) (2013) 529–540.
- [41] N. Chaput, S. Louafi, A. Bardier, F. Charlotte, J.C. Vaillant, F. Menegaux, et al., Identification of CD8+CD25+Foxp3+ suppressive T cells in colorectal cancer tissue, *Gut* 58 (4) (2009) 520–529.
- [42] Y. Kiniwa, Y. Miyahara, H.Y. Wang, W. Peng, G. Peng, T.M. Wheeler, et al., CD8+ Foxp3+ regulatory T cells mediate immunosuppression in prostate cancer, *Clin. Cancer Res.* 13 (23) (2007) 6947–6958.
- [43] S.M. Kaech, W. Cui, Transcriptional control of effector and memory CD8+ T cell differentiation, *Nat. Rev. Immunol.* 12 (11) (2012) 749–761.
- [44] O. Goldberger, I. Volovitz, A. Machlenkin, E. Vadai, E. Tzehoval, L. Eisenbach, Exuberant numbers of tumor-specific T cells result in tumor escape, *Cancer Res.* 68 (9) (2008) 3450–3457.
- [45] T. Lozano, S. Chocarro, C. Martin, A. Lasarte-Cia, C. Del Valle, M. Gorraiz, et al., Genetic modification of CD8(+) T cells to express EGFR: potential application for adoptive T cell therapies, *Front. Immunol.* 10 (2019) 2990.
- [46] D. Getnet, C.H. Marin, E.L. Hipkiss, J.F. Gross, T.J. Harris, H.R. Yen, et al., Tumor recognition and self-recognition induce distinct transcriptional profiles in antigen-specific CD4 T cells, *J. Immunol.* 182 (8) (2009) 4675–4685.